HAL
open science

Optimal control of a neuromusculoskeletal model: a second order sliding mode solution

Carlos Rengifo, Franck Plestan, Yannick Aoustin

To cite this version:

Carlos Rengifo, Franck Plestan, Yannick Aoustin. Optimal control of a neuromusculoskeletal model: a second order sliding mode solution. International Workshop on Variable Structure Systems, 2008., Jun 2008, Antalya, Turkey. pp.55 – 60, 10.1109/VSS.2008.4570682 . hal-00520405

HAL Id: hal-00520405

https://hal.science/hal-00520405v1

Submitted on 23 Sep 2010

HAL is a multi-disciplinary open access archive for the deposit and dissemination of scientific research documents, whether they are published or not. The documents may come from teaching and research institutions in France or abroad, or from public or private research centers.

L'archive ouverte pluridisciplinaire **HAL**, est destinée au dépôt et à la diffusion de documents scientifiques de niveau recherche, publiés ou non, émanant des établissements d'enseignement et de recherche français ou étrangers, des laboratoires publics ou privés.

Optimal control of a neuromusculoskeletal model: a second order sliding mode solution

Carlos Rengifo*, Franck Plestan*,x, and Yannick Aoustin*

*IRCCyN, Ecole Centrale de Nantes-Université de Nantes-CNRS, Nantes, France
x Corresponding author: Franck.Plestan@irccyn.ec-nantes.fr

***Abstract*—The objective in neuromusculoskeletal simulation consists in finding a set of muscles excitations in order to produce the desired motion and is an exciting challenge for medical operators. In this paper, muscle excitations are computed by using a second order sliding mode controller which is optimal with respect of a functional cost based on the tracking error and the torque square. The proposed strategy was tested using a two-dimensional human anthropomorphic arm composed of two joints and six muscles.**

I. Introduction

Computer simulation has become a very useful tool to investigate how the neuromusculoskeletal system interacts to produce coordinated motions and provides possibilities which are not generally possible by experimental ways. As a matter of fact, medical staff could use this simulator in order to evaluate the effect of their actions on a real patient or to analyze the behaviour of a patient who is deficient in his motion. Thus, individual muscular signals like neural excitations or forces can be perturbed in their incidence on the motion [6]. In this case, neuromusculoskeletal simulation is used to understand muscle coordination of human legs [19], to analyze normal and pathological gait [10] and to estimate muscle forces [2]. The role of closed loop control techniques in neuromusculoskeletal model simulation is crucial, as the following survey will display.

One of the formerly works in neuromusculoskeletal simulation [3] (forward dynamics simulation) consists in finding a set of muscles excitations which, when applied to forward dynamics equations, produces desired motions. In [1] the muscle excitations are taken as the optimization variables for minimizing the metabolic energy expended per traveled distance unit. This approach unfortunately is computationaly expensive: for example, muscle excitations computations for a 3D human walking model require more than 10000 hours of computation with a supercomputer [1]. Another proposition, called inverse dynamics [4], estimates muscle forces from joint torques, which are computed as a function of joint positions, velocities and accelerations. As muscles number is greater than joints number, different set of muscular forces could give the same joint torques. Several criteria have been proposed in order to solve the redundancy problem: among them, the minimum sum of muscle efforts [12], the minimum sum of muscle stresses [4] and the minimization of muscle work. Although inverse dynamics approach is a computationally efficient technique, its main drawback is its lack of robustness [14].

The second generation of neuromusculoskeletal simulation approaches is using closed-loop control strategies in order to compute muscular excitations. The controller input is the difference between desired and simulated motions, the output being muscle excitations vector. As stated in [13], the benefit of this tracking formulation is to constraint the model to produce more realistic results; however, the question on how neural central system is solving the redundancy problem still remains as an open problem. Three main strategies have been proposed, each one solving this redundancy problem by a different manner. In [16], computed muscle control is an extension of the computed torque control idea [8]: the minimization criteria is the square of euclidean norm of steady state muscular activations vector. Neuromusculoskeletal tracking [13] solves the redundancy problem using feedback linearization and linear quadratic control.

Recently, sliding mode control has been also applied to neuromusculoskeletal simulation. In [9], a strategy based on inverse dynamic and first order sliding mode control is used to track desired motion. The problem with first order sliding mode is that, before the system reachs the sliding surface, the insensitivity to variations of system parameters and external disturbances can not be ensured [17] and the convergence to origin is only asymptotic. The three aforementioned strategies solve in an effective way the tracking motion problem but use very artificial optimization criteria from physiological point-of-view. When desired motions are derived from experimental data, another shortcoming arises because in these works the desired movement is specified using positions, velocities and accelerations: however, it is well-known that second order time derivatives estimation of data signals is highly sensitive to noise.

The purpose of this paper is to present an application of second order sliding-mode techniques to neuromusculoskeletal simulation. As the used controller [11] is based on a high-order sliding mode approach [7], the robustness is ensured during the entire response as the sliding manifold is designed such that the system is evolving on this manifold early from initial time. Furthermore, the convergence time is finite and well-known in advance, and the reference trajectories are specified using only joint positions and velocities (and not accelerations, which is a positive point with respect to previous approaches), and the

minimization criteria for solving the redundancy problem has a strong physiological support.
The paper is organized as follows: The human arm model equations are given in Section II, as desired motions design. Section III describes the control strategy. Section IV presents the simulation results. The final section V contains conclusion and perspectives.

II. Anthropomorphic arm model

The driven system is depicted in Figure 1. The arm model is composed of 6 muscles and 2 joints and it is assumed the arm is evolving in a vertical plane.

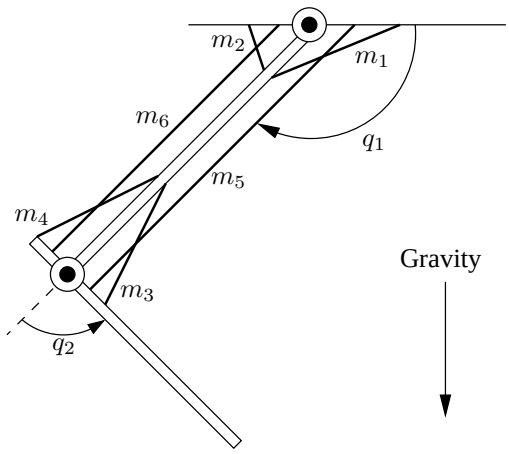

Fig. 1. Schematic representation of the human arm. The arm is moved by 6 muscles: 4 monoarticular ones (m_1, m_2, m_3 m_4) and 2 biarticular ones (m_5,m_6).

A. Skeletal dynamics

Using the second Lagrange method, skeletal dynamics equations are obtained

$$\mathbf{D}\left(q_2\right)\ddot{\mathbf{q}} + \mathbf{C}\left(\mathbf{q},\dot{\mathbf{q}}\right)\dot{\mathbf{q}} + \mathbf{G}(\mathbf{q}) + \tau_{\mathbf{f}}\left(\dot{\mathbf{q}}\right) = \mathbf{\Gamma} \tag{1}$$

with $\mathbf{q} = \begin{bmatrix} q_1 & q_2 \end{bmatrix}^T$ the generalized coordinates vector[1], $\mathbf{D}(q_2)(2\times 2)$ the symmetric positive inertia matrix, $\mathbf{C}(\mathbf{q},\dot{\mathbf{q}})(2\times 2)$ the Coriolis and centrifugal effects matrix and $\mathbf{G}(\mathbf{q})(2\times 1)$ the gravity effects vector. $\mathbf{\Gamma} = \begin{bmatrix} \Gamma_1 & \Gamma_2 \end{bmatrix}^T$ is the torques vector applied at the links joints and $\tau_{\mathbf{f}}\left(\dot{q}\right) = \begin{bmatrix} \tau_{f_1} & \tau_{f_2} \end{bmatrix}^T$ is the friction effects vector ($j = \{1,2\}$) such that $\tau_{f_j} = B_j\dot{q}_j + F_{s_j}\,\mathrm{sign}\left(\dot{q}_j\right)$. B_j and F_{s_j} are Coulomb and viscous friction coefficients for the considered links joint. Arm parameters are given in [15].

B. Torque-force relation

As no muscle is considered on the second link (Figure 1), relation between torques and forces is given by a constant matrix

$$\begin{bmatrix} \Gamma_1 \\ \Gamma_2 \end{bmatrix} = \underbrace{\begin{bmatrix} r_{11} & \dots & r_{16} \\ r_{21} & \dots & r_{26} \end{bmatrix}}_{\mathbf{R}} \cdot \begin{bmatrix} F_1 \\ \vdots \\ F_6 \end{bmatrix} \tag{2}$$

with F_i the force developped by muscle i. Coefficients of $\mathbf{R}$ matrix are given in [15].

C. Muscular forces

In the sequel, each muscle is supposed to be an instantaneously force generator, which means that the muscular force is a nonlinear algebraic function of the muscular activation $a(t)$. Furthermore, each tendon is supposed to be rigid, which means that its length is constant. Then, each muscle of the arm is characterized through the active muscular force which it is able to engender, this force being given from ($i = \{1,\cdots,6\}$)

$$F_{a_i} = a_i f_{l_i}\left(l_i\right) f_{v_i}\left(\dot{l}_i, v_{\max}\left(a_i, l_i\right)\right) F_{\max_i} \tag{3}$$

with l_i the length of muscle i, $F_{\max}$ the maximal value of muscular effort. The functions $f_l(.)$ and $f_v(.)$ and the parameters of the muscles are described in [15].

D. Musculo-skeletal geometry

Muscles are now linked to external supports. Of course, it means that their lengths depend on the articular positions. The relation between muscular fiber length and joint positions reads as

$$L = L_r - \mathbf{R}^T\left(q - Q_r\right) \tag{4}$$

$L = \begin{bmatrix} l_1 & \dots & l_6 \end{bmatrix}^T$ is the vector of muscular fiber lengths, $L_r = \begin{bmatrix} l_{r_1} & \dots & l_{r_6} \end{bmatrix}^T$ is the vector of muscle length in rest position, and and $Q_r = \begin{bmatrix} Q_{r_1} & Q_{r_2} \end{bmatrix}^T$ is the vector of rest position for every articular joint i. As the muscular force depends also on fiber length contraction velocity, the relation between these variables and joint velocities reads as $\dot{L} = -\mathbf{R}^T\dot{q}$.

E. Activation dynamics

The activations dynamics displays the relation between the muscular excitation u_i and the mechanical activation a_i and reads as

$$\dot{a}_i = \begin{cases} \left(u_i - a_i\right)\left[u_i/\tau_{a_i} + \left(1-u_i\right)/\tau_{d_i}\right], u_i \geq a_i, \\ \\ \left(u_i - a_i\right)/\tau_{d_i}, u_i < a_i, \end{cases} \tag{5}$$

with τ_{a_i} and τ_{d_i} respectively the time constants for the activation and desactivation dynamics. Excitation and activation levels are allowed to vary continuously between 0 and 1 [18].

[1]Notation ^{T} denote matrix transposition.

F. Simulation model

Simulation model is displayed in Figure 2 and is based on previous equations. Let x (resp. U) denote the state (resp. control input) vector: $x_s = \begin{bmatrix} x_{s_1} & \dots & x_{s_10} \end{bmatrix}^T = \begin{bmatrix} q_1 & \dot{q}_1 & q_2 & \dot{q}_2 & a_1 & \dots & a_6 \end{bmatrix}^T$, $U = \begin{bmatrix} u_1 & \dots & u_6 \end{bmatrix}^T$. Then, the arm model reads as a nonlinear system which is not affine in control input,

$$\dot{x}_s = \bar{f}\left(x_s, U\right) \tag{6}$$

As as matter of fact, the system can not be written as a nonlinear model affine in U (which would be more convenient for control design) because activation dynamics (5) depends on u_i and u_i^2. As the objectice consists in forcing the arm to track articular positions trajectories, the system output is defined as $y = \begin{bmatrix} x_1 & x_3 \end{bmatrix}^T$.

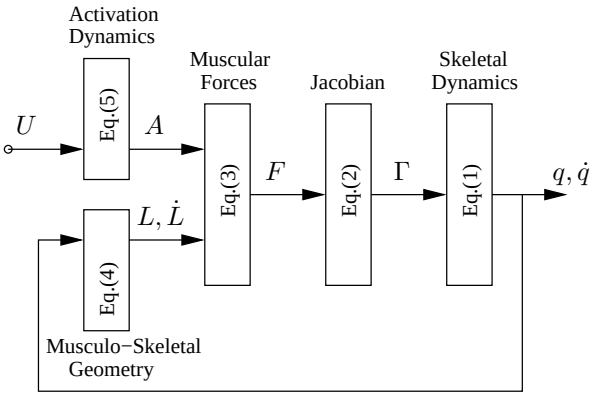

Fig. 2. Elements of human arm musclen driven simulation. $U = [u_1 \cdots u_6]^T$ is the muscular excitations vector (and then the control input vector). $A = [a_1 \cdots a_6]^T$ is the muscular activations vector. $F = [F_{a_1} \cdots F_{a_6}]^T$ is the active muscular forces cvector. $L = [l_1 \cdots l_6]^T$ is the muscular fiber length vector. $\Gamma = [\Gamma_1 \;\; \Gamma_2]^T$ is the joint torques vector. $q = [q_1 \;\; q_2]^T$ is the joint positions vector.

G. Control synthesis model

Muscle dynamics are stable [2] and faster than arm motions, which yields that muscle dynamics can be neglected. Then, the model, which will be used for control design, is built by supposing that there is no dynamics between A and U (see Figure 2), *i.e.* $A = U$. Then, the system can be written as

$$\dot{x} \;=\; f(x) + g(x)U \tag{7}$$

with $x = \begin{bmatrix} x_1 & \dots & x_4 \end{bmatrix}^T = \begin{bmatrix} q_1 & \dot{q}_1 & q_2 & \dot{q}_2 \end{bmatrix}^T$, $U = \begin{bmatrix} u_1 & \dots & u_6 \end{bmatrix}^T$.

[2]Equations (5) are linear in a_i. Then, it is easy to find an analytic solution for a_i and to show that it is a BIBO (bounded input bounded output) stable system.

III. Control strategy

The proposed control strategy is a hierarchical one composed by four levels (Figure 3), the output of each level being a reference signal for the next one. It is recalled that the control objective consists in tracking articular reference trajectoire $q_{r_i}(t)$ by acting through the excitation of the six muscles (through input U). An other objective consists also in designing robust controller with respect to parameters variations (for example, mass which would be adding on the forarm as an object taking in the hand).

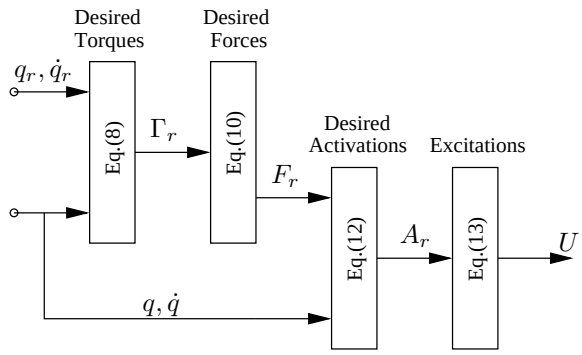

Fig. 3. Proposed control scheme.

A. Control scheme

The four levels of the controller scheme can be detailed as follows:

First level. This block computes the desired torques Γ_r using computed-torque formulation (8) and robust control (9)

$$\Gamma_r = \hat{\mathbf{D}}\left(q_2\right)\eta + \hat{\mathbf{C}}\left(q, \dot{q}\right)\dot{q} + \hat{\mathbf{G}}(q) + \hat{\tau}_{\mathbf{f}}\left(\dot{q}\right) \tag{8}$$

$$\eta = \begin{bmatrix} \eta_1 & \eta_2 \end{bmatrix}^T := f_c\left(q_r, \dot{q}_r, q, \dot{q}\right) \tag{9}$$

with $\hat{\mathbf{D}}$, $\hat{\mathbf{C}}$, $\hat{\mathbf{G}}$, $\hat{\tau}_{\mathbf{f}}$ the estimated values of $\mathbf{D}$, $\mathbf{C}$, $\mathbf{G}$ and $\tau_{\mathbf{f}}$ (1) (knowing that these terms have uncertainties). In Section III-B, a solution for η based on second order sliding mode controller is proposed and compared (in simulation) with a classical proportional-derivative control. Note that these both controllers are computed in order to minimize a criteria such that the torques are minimal.

Second level. Desired muscular forces $F_r = \begin{bmatrix} F_{a_{1_r}} & \dots & F_{a_{6_r}} \end{bmatrix}^T$ are computed as a function of desired torques using the linear relation (from equation (2))

$$\Gamma_r \;=\; \mathbf{R}F_r. \tag{10}$$

This system having six unknowns and two equations, there exists an infinity of exact solutions. As a consequence, vector F_r is chosen in order to minimize muscle efforts. Then, at each simulation step, the following constrained optimization problem is solved using linear programming

$$\min_{F_{a_{i_r}}>0} \quad \sum_{i=1}^{6} \left(\frac{F_{a_{i_r}}}{F_{\max_i}}\right)^2 \tag{11}$$

with $F_{\max_i}$ being the maximum value allowed for muscle i (for numerical values, see [15]).

Third level. Desired activations $A_r = \begin{bmatrix} a_{1_r} & \dots & a_{6_r} \end{bmatrix}^T$ are computed in order to obtain desired forces vector F_r. For each muscle, a_{r_i} ($i = \{1 \dots 6\}$) is obtained as a function of $F_{a_{ir}}$ using contraction dynamics (3). For a sake of clarity, equation (3) is rewritten for each muscle i by using the reference activations (with $i = \{1 \dots 6\}$)

$$F_{a_{ir}} = a_{r_i} F_l\left(l_i\right) F_{v_i}\left(\dot{l}_i, v_{\max}\left(a_{r_i}, l_i\right)\right) F_{\max_i} \tag{12}$$

In this case, one gets a system with six unknowns and six independent nonlinear equations. Find an explicit solution for a_{r_i} is a hard task: solutions of system (12) are numerically calculated by using a root solver.

Fourth level. Muscle excitations input vector $U = \begin{bmatrix} u_1 & \dots & u_6 \end{bmatrix}^T$ is computed as a function of the desired activations. Given the activation dynamics equation (5), for a constant excitation $u(t) = \bar{u}$, the corresponding steady-state activation $\bar{a}$ equals $\bar{u}$. Thus, excitation inputs are computed by using the trivial equation (with $i = \{1 \dots 6\}$)

$$u_i = a_{r_i}. \tag{13}$$

B. Robust controller

In this section, two different controllers are presented. The first one is based on a second order sliding mode control approach, the second one using a proportional-derivative control and being designed in order to offer performances comparisons with respect to the previous one. The both controllers are *synthetized* from model displayed in Section II-G whereas they are *evaluated* on a simulator based on the model displayed in Section II-F. Controller parameters are determined by minimization of the following performance index

$$J = \int_0^{t_f} \left[\left(q - q_r\right)^T \left(q - q_r\right) e^t + \Gamma^T Q \Gamma \right] \, \mathrm{d}t \tag{14}$$

with

$$\Gamma^T Q \Gamma = \left(\frac{\Gamma_1}{\Gamma_{ss_1}}\right)^2 + \left(\frac{\Gamma_2}{\Gamma_{ss_2}}\right)^2$$

The exponential term e^t gives a strong weight to tracking errors in latter time interval. The weight matrix Q was chosen to penalize large control signals. Q allows to compare each joint torque with respect to its steady-state value. $\Gamma_{ss} = \begin{bmatrix} \Gamma_{ss_1} & \Gamma_{ss_2} \end{bmatrix}^T = G\left(q_f\right)$ is obtained by evaluating skeletal dynamics at $t = t_f$ ($q\left(t_f\right) = q_f$, $\dot{q}\left(t_f\right) = 0$, $\ddot{q}\left(t_f\right) = 0$).

C. Sliding mode control

The feedback control (9) is defined by the second-order integral sliding control law proposed by [11]. Let s_i ($i = \{1, 2\}$) denote the so-called sliding variable defined as $s_i = q_i - q_{r_i}(t)$. The objective of a second order sliding mode controller consists in forcing the system to track trajectories such that, in finite time and in spite of uncertainties, one has $s_i = \dot{s}_i = 0$ for $t > t_c$.

1) Some recalls: Define $s = \begin{bmatrix} s_1 & s_2 \end{bmatrix}^T$. From (1) and (8) one gets,

$$\begin{aligned} \ddot{s} &= \ddot{q} - \ddot{q}_r(t) \\ &= \mathbf{D}^{-1}\left(q_2\right) \Big[\hat{\mathbf{D}}\left(q_2\right) \eta + \hat{\mathbf{C}}\left(q, \dot{q}\right) \dot{q} + \hat{\mathbf{G}}(q) + \\ &\qquad \hat{\tau}_{\mathbf{f}}\left(\dot{q}\right) - \mathbf{C}\left(q, \dot{q}\right) \dot{q} - \mathbf{G}(q) - \tau_{\mathbf{f}}\left(\dot{q}\right) \Big] - \ddot{q}_{r_i}(t) \\ &:= \chi(\cdot) + \beta(\cdot)\eta \end{aligned} \tag{15}$$

H1. The solutions of (15) are understood in the Filippov sense [5], and system trajectories are supposed to be infinitely extendible in time for any bounded Lebesgue measurable input.

H2. β is a dominant diagonal matrix for $x \in \mathbf{X} \subset I\!R^4$, $\mathbf{X}$ being a bounded open subset of $I\!R^4$ within which the boundedness of the system dynamics is ensured.

Last assumption implies that system (15) is "sufficiently" decoupled which allows to consider that input η_i is acting on sliding variable s_i and then to design by a separate way each component of input vector. Then, for a sake of clarity, one supposes only the case of monovariable system. Consider now single input equation

$$\ddot{s}_i \quad = \quad \chi_i(\cdot) + \beta_i(\cdot)\eta_i \tag{16}$$

H3. Functions $\chi_i(\cdot)$ and $\beta_i(\cdot)$ are bounded uncertain functions, and, without loss of generality, let also the sign of the control gain β_i be constant and strictly positive. Thus, there exist $K_m \in I\!R^{+*}$, $K_M \in I\!R^{+*}$, $C_0 \in I\!R^+$ such that

$$0 < K_m < \beta_i < K_M \quad |\chi_i| \leq C_0. \tag{17}$$

for $x \in \mathbf{X}$.

The synthesis of a high order sliding mode controller for (16) is made through the following idea: switching variable is defined such that the system evolves, *early from* $t = 0$, on a switching manifold. Furthermore the sliding variable and its time derivatives reach the origin in finite time in spite of uncertainties thanks to discontinuous control input. The design of the controller consists in two steps

- Design of the switching variable for system (16),
- Design of a discontinuous control input η_i maintaining the system trajectories on the switching manifold which ensures the establishment of a second order sliding mode, in spite of uncertainties.

Switching variable. Let S_i denote the switching variable defined as

$$S_i \quad = \quad \dot{s}_i - \dot{\mathcal{F}}_i(t) + \lambda_{0_i}\left[s_i - \mathcal{F}_i(t)\right], \tag{18}$$

with $\lambda_{0_i} > 0$. The function $\mathcal{F}_i(t)$, called *pre-computed trajectory*, is at least a C^2-one defined such that $S_i(t = 0) = 0$ and $s_i^{(k)}(t = t_c) - \mathcal{F}_i^{(k)}(t_c) = 0$ ($k = \{0, 1\}$). Then, from initial and final conditions, the problem consists in finding the function $\mathcal{F}_i(t)$ such that

$$\begin{aligned} s_i(t = 0) &= \mathcal{F}_i(0), & s_i(t = t_c) &= \mathcal{F}_i(t_c) = 0, \\ \dot{s}_i(t = 0) &= \dot{\mathcal{F}}_i(0), & \dot{s}_i(t = t_c) &= \dot{\mathcal{F}}_i(t_c) = 0 \end{aligned} \tag{19}$$

A solution for $\mathcal{F}_i(t)$ reads as

$$\mathcal{F}_i(t) \quad = \quad a_{3,i}t^3 + a_{2,i}t^2 + a_{1,i}t + a_{0,i} \qquad (20)$$

H4. There exists a finite positive constant $\Theta_i \in I\!R^+$ such that, for $0 \leq t \leq t_c$,

$$\ddot{s}_i - \ddot{\mathcal{F}}_i(t) + \lambda_{0_i}\left[\dot{s}_i - \dot{\mathcal{F}}_i(t)\right] \quad < \quad \Theta \qquad (21)$$

Equation $S_i = 0$ describes the desired dynamics which satisfy the finite time stabilization of vector $[\dot{s}_i \;\; s_i]^T$ to zero. Then, the *switching manifold* on which system (16) is forced to slide on via a discontinuous control η_i, is defined as

$$\mathcal{S}_i \quad = \quad \{x \mid S_i = 0\} \qquad (22)$$

Given equation (19), one gets $S_i(t = 0) = 0$: at the initial time, the system still evolves on the switching manifold.

Controller design. The attention is now focused on the design of the discontinuous control law u which forces the system trajectories of (16) to slide on $\mathcal{S}_i$, to reach in finite time the origin and to maintain the system at the origin.

Theorem 1: [11] Consider the nonlinear system (16) with a relative degree 2 with respect to $s_i(x,t)$. Suppose that it is minimum phase and that hypotheses H_1, H_2, and H_3 are fulfilled. Let 2 be the sliding mode order and $0 < t_c < \infty$ the desired convergence time. Define $S_i \in I\!R$ by

$$S_i \quad = \quad \begin{cases} \dot{s}_i - \dot{\mathcal{F}}_i(t) + \lambda_{0_i}\left[s_i - \mathcal{F}_i(t)\right] & 0 \leq t < t_c \\ \dot{s}_i + \lambda_{0_i} s_i & t \geq t_c \end{cases} \qquad (23)$$

with pre-computed trajectory derived from (19) such that assumption H4 is fulfilled. The control input η_i defined by

$$\eta_i \quad = \quad -k_i \,\mathrm{sign}(S_i) \qquad (24)$$

with

$$k_i \quad \geq \quad \frac{C_0 + \Theta + \epsilon}{K_m}, \qquad (25)$$

C_0, K_m defined by (17), Θ defined by (21), $\epsilon > 0$, leads to the establishment of a second order sliding mode with respect to s_i. The convergence time is t_c. ■

Sketch of proof. Condition (25) allows to satisfy the η-attractivity condition $\dot{S}S \leq -\epsilon|S|$. For more details, see [11].

2) Application: $\mathcal{F}_i(t) = a_{3,i}t^3 + a_{2,i}t^2 + a_{1,i}t + a_{0,i}$ is computed such that $\mathcal{F}_i(0) = e_i(0)$, $\mathcal{F}_i(t_c) = 0$, $\dot{\mathcal{F}}_i(0) = \dot{e}_i(0)$, $\dot{\mathcal{F}}_i(t_c) = 0$. Parameters t_c, λ_{0_1} and λ_{0_2} are determined by minimization of the performance index (14) after setting $k_1 = 20$ and $k_2 = 30$. The obtained values are $\lambda_{0_i} = 17.81$, $t_c = 4.8$, $a_{3,i} = 0.0142$, $a_{2,i} = -0.10230$, $a_{1,i} = 0$, $a_{0,i} = 0.7854$ $(i = 1, 2)$.

D. Proportional-derivative control

In order to evaluate performances (and its interest versus a "classical" controller) of previous second order sliding mode controller, the feeedback control law (9) reads as a proportional-derivative control equation (with $s_i(t) = q_i(t) - q_{r_i}(t)$, $i = \{1, 2\}$) $\eta_i = k_p s_i + k_d \dot{s}_i$. Parameters k_p and k_d are determined by minimization of the performance index (14) which gives $k_p = 18.2070$, $k_d = 0.1774$.

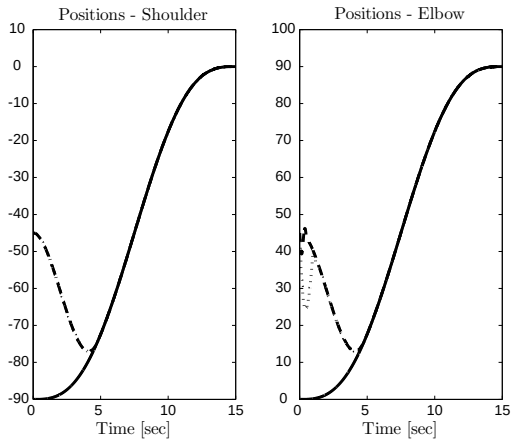

Fig. 4. **Second order sliding mode control.** Joint positions (deg) versus time (sec): trajectory reference (solid line), nominal case (dashed line) and uncertain case (+50% mass error) (dotted line).

IV. Simulations

In this section simulation results are displayed. In order to evaluate control performance and robustness versus parameters variations, two sets of simulation have been made: the first one is made by supposing that all parameters are fully well-known (called "nominal case"), whereas the second one supposes an error in the upper-arm mass of 50% (called "uncertain case"). For the second order sliding mode control, positions, torques and excitations for both nominal and uncertain cases are respectively displayed in Figures 4, and 5, whereas, for PD control, results are compared in Figures 6 and 7. These simulations clearly show that second order sliding mode controller is more robust to mass variations than PD one: furthermore, the finite time feature of second order sliding mode control clearly appears.

V. Conclusion and perspectives

A new neuromusculoskeletal simulation technique based on second-order sliding mode control has been proposed. It allows to evaluate, under optimal criteria as minimum sum of muscle efforts, muscle activations in order to move an human-equivalent arm under a prescribed planar motion. From the control point-of-view, simulations have shown that the closed-loop system is robust versus mass variations. Furthermore, in spite of difference between control synthesis model and simulation model (muscle activation dynamics are neglected for control design), tracking error converges towards zero in an arbitrary fixed time t_c. This latter time is limited only by physical constraints [18] as muscle activation $u_i(t)$ must be such that $(0 \leq u_i(t) \leq 1)$. Futher works consist in applying a such strategy on a biped model in order to simulate human gait

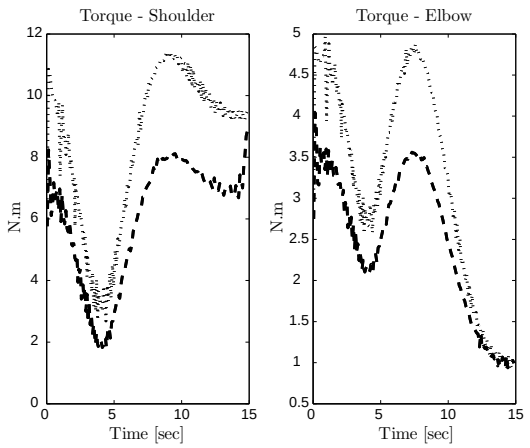

Fig. 5. **Second order sliding mode control.** Torques ($N \cdot m$) versus time (sec): nominal case (dashed line) and uncertain case (+50% mass error) (dotted line).

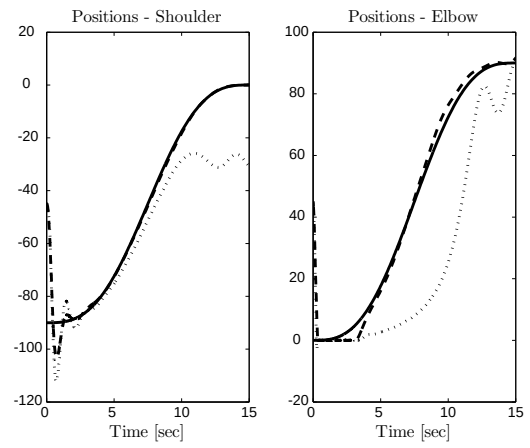

Fig. 6. **PD control.** Joint positions (deg) versus time (sec): trajectory reference (solid line), nominal case (dashed line) and uncertain case (+50% mass error) (dotted line).

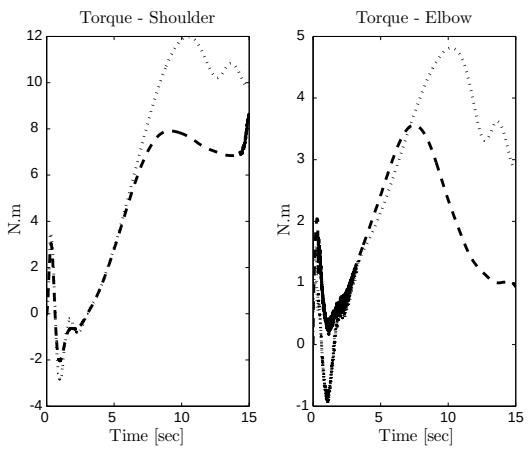

Fig. 7. **PD control.** Torques ($N \cdot m$) versus time (sec): nominal case (dashed line) and uncertain case (+50% mass error) (dotted line).

and to obtain medical staffs simulators usable for pathology diagnostic or operation consequences.

ACKNOWLEDGMENT

Carlos Rengifo would like to thank Cauca University (Colombia) for his financial support.

REFERENCES

[1] F. Anderson and M. Pandy, "Dynamic optimization of human walking," *Journal of Biomechanical Engineering*, vol. 123, pp. 381–390, 2001.

[2] T. Buchanan, D. Lloyd, K. Manal, and T. Besier, "Neuromusculoskeletal modeling: Estimation of muscle forces and joint moments and movements from measurements of neural command," *Journal of Applied Biomechanics*, vol. 20, no. 4, pp. 367–395, November 2004.

[3] C. Chow and D. Jacobson, "Studies of human locomotion via optimal programming," *Mathematical Biosciences*, vol. 10, no. 3–4, pp. 239–306, April 1971.

[4] R. Crowninshield and R. A. Brand, "A physiologically based criterion of muscle force prediction in locomotion," *Journal of Biomechanics*, vol. 14, no. 11, pp. 793–801, 1989.

[5] A. Filippov, *Differential equations with discontinuous right-hand side*. Kluwer – Netherland: Dordrecht, 1988.

[6] T. Komura, A. Nagano, H. Leung, and Y. Shinagawa, "Simulating pathological gait using the enhanced linear inverted pendulum model," *IEEE Transaction on Biomedical Engineering*, vol. 52, no. 9, pp. 1502–1513, September 2005.

[7] A. Levant, "Sliding order and sliding accuracy in sliding mode control," *International Journal of Control*, vol. 58, no. 6, pp. 1247–1263, 1993.

[8] F. Lewis, C. Abdallah, and D. Dawson, *Control of Robot Manipulators*. New York – USA: Macmillan Publishing Company, 1993.

[9] S. Lister, N. Jones, S. Spurgeon, and J. Scott, "Simulation of human gait and associated muscle activation strategies using sliding-mode control techniques," *Simulation Modelling Practice and Theory*, vol. 14, no. 5, pp. 586–596, July 2006.

[10] S. Piazza, "Muscle-driven forward dynamic simulations for the study of normal and pathological gait," *Journal of NeuroEngineering and Rehabilitation*, vol. 3, no. 5, pp. 1–7, March 2006.

[11] F. Plestan, A. Glumineau, and S. Laghrouche, "A new algorithm for high order sliding mode control," *International Journal of Robust and Nonlinear Control*, vol. 18, no. 4-5, pp. 441–453, March 2006.

[12] A. Seireg and R. Arvikar, *Biomechanical Analysis of the Musculoskeletal Structure for Medicine and Sports*. Hemisphere Publishing Corporation, 1989.

[13] A. Seth and M. Pandy, "A neuromusculoskeletal tracking method for estimating individual muscle forces in human movement," *Journal of Biomechanics*, vol. 40, no. 2, pp. 356–366, 2007.

[14] M. Silva and J. Ambrósio, "Sensitivity of the results produced by the inverse dynamic analysis of a human stride to perturbed input data," *Gait & Posture*, vol. 19, no. 1, pp. 35–49, February 2004.

[15] S. Stroeve, "Impedance characteristics of a neuromusculoskeletal model of the human arm i: Posture control," *Biological Cybernetics*, vol. 81, no. 5–6, pp. 475–494, Novembre 1999.

[16] D. G. Thelen, F. C. Anderson, and S. L. Delp, "Generating dynamic simulations of movement using computed muscle control," *Journal of Biomechanics*, vol. 36, no. 3, pp. 321–328, March 2003.

[17] V. Utkin and J. Shi, "Integral sliding mode in systems operating under uncertainty conditions," in *Conference on Decision and Control*, Kobe, Japan, December 1996, pp. 4591–4596.

[18] F. Zajac, "Muscle and tendon: properties, models, scaling, and application to biomechanics and motor control," *Critical Reviews in Biomedical Engineering*, vol. 17, no. 4, pp. 359–411, 1989.

[19] ——, "Understanding muscle coordination of the human leg with dynamical simulations," *Journal of Biomechanics*, vol. 35, no. 8, pp. 1011–1018, August 2002.